Antirelaxation coatings in coherent spectroscopy: Theoretical investigation and experimental test

K. Nasyrov,[1] S. Gozzini,[2,*] A. Lucchesini,[2] C. Marinelli,[2,3] S. Gateva,[4] S. Cartaleva,[4] and L. Marmugi[2,5]

[1]*Institute of Automation and Electrometry SB RAS, Novosibirsk, Russia*

[2]*Istituto Nazionale di Ottica del CNR – UOS Pisa, Via Moruzzi 1, 56124 Pisa, Italy*

[3]*DSFTA, Università di Siena, Via Roma 56, 53100 Siena, Italy*

[4]*Institute of Electronics, BAS, boul. Tzarigradsko shosse 72, 1784 Sofia, Bulgaria*

[5]*Department of Physics and Astronomy, University College London, Gower Street, London WC1E 6BT, United Kingdom*

(Received 7 May 2015; published 2 October 2015)

We describe a theoretical model, based on a density matrix and the Liouville equation, for the investigation of magneto-optical resonances in alkali-metal atomic vapor, in particular in the case of the electromagnetically induced transparency (EIT) in the presence of antirelaxation coatings. The influence of the coating is parametrized with an empirical coefficient describing its efficiency; the calculations are extended to a broad range of coating quality, contrary to previous works, and to uncoated cells. The model takes into account also different configurations for the EIT formation and different efficiency of optical pumping, as determined by the coating characteristics and the atomic energy structure. The model is validated by investigating the EIT with degenerate Zeeman levels in ^{39}K D_1 and Cs D_2 lines, which exhibit respectively an almost negligible and a relevant impact of hyperfine optical pumping. The results are compared to experimental data, exhibiting good agreement; in particular, for the ^{39}K D_1 line, recent findings are shown here in the case of degenerate and nondegenerate EIT with amplitude-modulated light. Our results demonstrate an effective approach for the investigation of antirelaxation coatings and their contribution in the formation of magneto-optical resonances in alkali-metal atoms, in different regimes and with largely different efficiencies. This sheds new light on well-known but not yet entirely clarified phenomena and their behavior as a function of experimental parameters.

DOI: 10.1103/PhysRevA.92.043803 PACS number(s): 42.50.Gy, 32.80.Qk, 42.50.Ct, 42.70.Jk

I. INTRODUCTION

Antirelaxation coatings in optical cells are recognized effective tools to reduce the depolarization and adsorption of atoms after collisions against the glass walls, thus decreasing losses due to optical pumping. Indeed, organic coatings have been successfully employed in numerous different experiments; for example, for light-induced diffusion of atoms and molecules [1], light-induced desorption of weakly bound adsorbed atoms [2,3], and for coherent spectroscopy [4], cold and ultracold atom experiments [5–7], ultrasensitive optical atomic magnetometers [8,9], and atomic clocks [10].

In fact, by coating the vapor cell walls with antirelaxation polymers, it is possible to preserve the atomic spin orientation after many atom-wall collisions: the collision becomes elastic and, hence, does not affect the internal degrees of freedom of the atom. Paraffin coatings can support approximately up to 10^4 collisions without depolarization of the alkali-metal atom spins; in particular, specially designed coatings allow up to 10^6 atom-wall collisions without spin relaxation [11]. Nevertheless, the details of the antirelaxation coating's influence on the characteristics of the magneto-optical resonances in alkali-metal vapors are neither entirely understood nor theoretically described in actual experimental configurations.

In this paper, we present a theoretical model based on the Liouville equation formalism for the atomic density matrix, conceived for the description of the influence of antirelaxation coatings on the characteristics of the electromagnetically induced transparency (EIT) resonances observed in alkali-metal atoms. The model is suitable for the case of highly efficient coatings, which was practically unfeasible within the previous approaches [12]. In order to demonstrate the validity of the theoretical description, results are compared to the experimental outcomes of coherent spectroscopy experiments in Cs [13] and K [14]: our model indeed reproduces very well the experimental features of the EIT resonances, obtained with the degenerate Zeeman sublevels. In this case, the EIT resonance is observed as a function of the applied magnetic field at $B = 0$, when the degenerate magnetic levels of alkali-metal atoms are coupled by an unmodulated resonant laser beam.

In particular, in the case of ^{39}K vapor contained in a glass cell coated with polydimethylsiloxane (PDMS), the model successfully reproduces and explains the significant enhancement of the coherent resonance contrast [14]. In addition, the agreement with the observed results proves that our model can reproduce different levels of optical pumping efficiency. In fact, it is worth recalling here that in the case of Cs D_2 lines, the two hyperfine optical transition groups arising from the $F = 3,4$ ground states are well separated: the ground-state hyperfine splitting is 9.2 GHz, therefore larger than the Doppler width at room temperature (350 MHz). As a consequence, hyperfine optical pumping is highly effective, resulting in an almost complete depletion of the levels excited by the laser light. On the contrary, in ^{39}K, the D_1 line hyperfine transitions starting from the ground states $F = 1,2$ are almost completely overlapped: their separation is 462 MHz, while the Doppler broadening at room temperature is about 765 MHz. This produces an effective repumping mechanism, which effectively reduces the impact of the optical pumping [14].

Finally, in the case of ^{39}K, EIT resonances produced with nondegenerate Zeeman sublevels coupled by amplitude-modulated light will be presented. In this configuration, EIT resonances are observed at nonzero magnetic field, when the

*silvia.gozzini@ino.it

frequency of the amplitude modulation of the resonant light matches the Larmor frequency of the atoms.

II. THEORETICAL MODEL

To describe the dynamics of atom-light interactions in cells containing only alkali-metal vapor and without any antirelaxation coating, one can consider that atoms penetrating the laser beam equally populate the ground-state Zeeman sublevels. This implies an isotropic distribution of the atomic spin orientation and, therefore, no alignment of the atomic vapor. This derives from the assumption that the atom collisions with the glass cell walls cause a complete relaxation of the atomic polarization, or, in other words, a random redistribution of the population among all the Zeeman components of the ground-state hyperfine levels.

As a consequence of the interaction with the resonant polarized light, however, the angular momenta of atoms crossing the laser beam are anisotropically oriented, and a fraction of them is optically pumped to the ground-state hyperfine level noninteracting with the laser light. Nevertheless, after collisions with the bare glass cell walls, the atomic orientation is destroyed and all the magnetic sublevels of the ground-state levels are equally populated. Therefore, when the atoms re-enter the laser beam, they can be considered completely unpolarized.

Instead, in the case of glass cells with antirelaxation coatings, the atoms maintain the orientation imposed by the interaction with light after the collisions against the coated walls. As a consequence, they can interact again with the laser light without any modification of their internal state: atoms can therefore re-enter the laser beam with a nonuniform population distribution due to the pre-existent alignment. Thus, the initial conditions for the atoms re-entering the laser beam depend on the previous interactions with the resonant light and hence on the quantum state where they have been forced on. This was demonstrated to be effective in improving the contrast and in providing a Ramsey-like narrowing of the EIT resonances in many different experimental configurations [15].

The dependence on the previously occupied quantum state is expressed mathematically by an integrodifferential equation [16], whose solution can be found by iterations. According to this approach, the number of iterations needed for the convergence is proportional to the number N of collisions of a single atom with the walls without a spin change, or, equivalently, the inverse of the collisional depolarization rate ε: $N = 1/\varepsilon$. Hence, for high-quality antirelaxation coatings, a very large number of iterations is necessary. For this reason, in practice it is not possible to perform calculations for cells with coatings that allow more than $N = 10$ collisions without spin depolarization, i.e., only values $\varepsilon \geqslant 0.1$ can be taken into account [16].

Here we present an effective method to overcome this limitation: an approach is demonstrated to allow the solution even for very small values of ε. In detail, if we consider a cylindrical optical cell longer than the radius (Fig. 1), then the collisions of the atoms with the two optical windows are significantly less frequent than the ones against the lateral surface and, therefore, can be neglected. In addition, if the laser beam propagates along the optical cell axis, the density matrix $\rho(u,r)$ describing the atomic internal state has a cylindrical

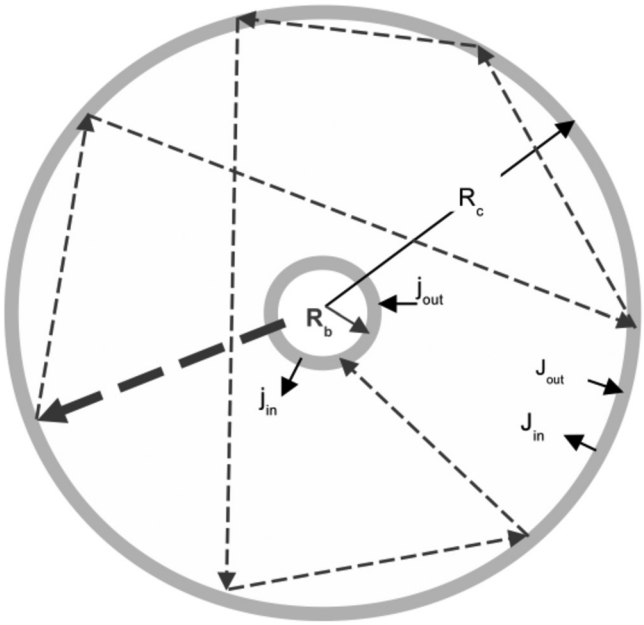

FIG. 1. Cross-section of the optical cell used for modeling the light-atom interaction. The central circle represents the cross-section of the laser beam. Dashed lines illustrate a possible random path of atom between two subsequent interactions with the laser beam. J_{out} and J_{in} are the atoms flux towards the walls and backwards respectively. j_{out} and j_{in} are the atomic fluxes entering and exiting the laser beam, respectively.

symmetry. Here u is the radial velocity of an atom and r its distance from the cell axis.

In this context, the evolution of the density matrix is described by the Liouville equation [17]

$$\frac{\partial}{\partial t}\rho(u,r) + \frac{1}{r}\frac{\partial}{\partial r}ru\rho(u,r) + (\hat{L}_0 + \hat{L}_H + \hat{L}_E)\rho(u,r) = 0, \tag{1}$$

where the operator $\hat{L}_0$ describes the atomic inner state evolution, including relaxation as well as the spontaneous emission; $\hat{L}_H$ describes the atom interaction with the constant external magnetic field, assumed uniform along all the interaction region, and $\hat{L}_E$ describes the atom interaction with the electric field of the resonant optical radiation.

By integrating this equation over the cross section S, which describes the free volume of the cell outside the laser beam (Fig. 1), the following equation is obtained:

$$\frac{d}{dt}\bar{\rho} + \hat{L}_H\bar{\rho} + \frac{2\pi R_c}{S}(J_{\text{out}} - J_{\text{in}}) + \frac{2\pi R_b}{S}(j_{\text{out}} - j_{\text{in}}) = 0. \tag{2}$$

In Eq. (2), R_c is the cell radius and R_b the laser beam radius. Accordingly, the cell cross section not occupied by the laser beam can be easily expressed as $S = \pi(R_c^2 - R_b^2)$. $\bar{\rho}$ is the density matrix averaged over the atomic velocity and the cell volume not occupied by the laser beam.

As sketched in Fig. 1, J_{out} represents the flow of atoms colliding against the cell walls and J_{in} is the reverse flow of atoms coming back from the walls into the cell free volume. Similarly, j_{out} and j_{in} indicate the flows of atoms entering and exiting the laser beam, respectively.

In this situation, the contribution of the antirelaxation coating is to let the atoms experience many collisions against the cell wall without losing their alignment. Therefore, an atom re-enters the cell volume occupied by the laser beam still maintaining the polarization previously imposed by the interaction with the laser light and the magnetic field. The limit condition, which reproduces the effect of a highly efficient antirelaxation coating, occurs when atoms coming out from the laser beam experience many collisions against the cell walls before re-entering the interaction region. Indeed, in this case the effect of the antirelaxation coating is maximized. Therefore, in the following, the case $R_c \gg R_b$ which implies $\frac{\pi}{2}\frac{R_c}{R_b} \gg 1$, is treated in detail. It is important to emphasize that this expression takes into consideration the average number of atom-wall collisions before a new crossing of the laser beam by an atom.

It is assumed that at each collision with the cell wall the atom thermalizes; this means that, on average, the atomic velocity of the "bouncing" atoms is described by the Maxwell-Boltzmann distribution at the temperature of the cell. In addition, the distribution of the atomic internal state in the cell free volume approaches the average value over the cell, if atoms spend enough time out of the laser beam volume. This allows us to postulate that the density matrix describing an atom outside the laser beam is equal to

$$\rho = \frac{e^{-(\mathrm{v}^2/\mathrm{v}_T^2)}}{\sqrt{\pi}\,\mathrm{v}_T^3}\bar{\rho}, \tag{3}$$

and hence $J_{\mathrm{out}} = j_{\mathrm{out}} = \mathrm{v}_T\bar{\rho}$, where v_T is the atom thermal velocity.

For each atom–coated-wall collision, there is a probability ε for thermalization of the atomic internal degrees of freedom. By this way, the flux of atoms coming from the walls can be written as

$$J_{\mathrm{in}} = (1-\varepsilon)\mathrm{v}_T\bar{\rho} + \varepsilon\mathrm{v}_T\rho_0, \tag{4}$$

where ρ_0 is the atomic density matrix in equilibrium, i.e., when all magnetic sublevels of the ground state are equally populated.

Provided that the intensity distribution of the laser beam is uniform, the solution of the Liouville equation (1) can be recast as

$$\rho = e^{-(\hat{L}_0+\hat{L}_H+\hat{L}_E)\tau_b}\bar{\rho}. \tag{5}$$

Here τ_b is the time that an atom spends inside the laser beam, which can be assumed, for simplicity, of the order of $\tau_b = R_b/\mathrm{v}_T$. Also in Eq. (5), we assume that the initial density matrix of the atoms entering the laser beam is equal to the average density matrix of the atoms outside the laser beam $\bar{\rho}$. Hence, the atomic flux coming from the laser beam is given by

$$j_{\mathrm{in}} = \mathrm{v}_T e^{-(\hat{L}_0+\hat{L}_H+\hat{L}_E)\tau_b}\bar{\rho}. \tag{6}$$

If we consider Eqs. (3), (4) and (6), then Eq. (2), in steady-state condition, can be written as

$$\left[\tau_c\hat{L}_H + \varepsilon + \frac{R_b}{R_c}(1 - e^{-(\hat{L}_0+\hat{L}_H+\hat{L}_E)\tau_b})\right]\bar{\rho} = \varepsilon\rho_0, \tag{7}$$

where

$$\tau_c = \frac{R_c^2 - R_b^2}{2\mathrm{v}_T R_c} \approx \frac{R_c}{2\mathrm{v}_T} \tag{8}$$

is the typical lifetime of the atom between two consequent collisions against the cell wall. Equation (7) can be solved numerically in order to obtain the averaged density matrix $\bar{\rho}$, which should be used as the initial density matrix for atoms crossing the laser beam. The numerical methods for simulating the atom flux dynamic inside the laser beam are described in Refs. [16–18] (see also Appendix).

A. Hanle resonances in alkali-metal atoms

We apply the described approach to the investigation of EIT resonances in the Hanle configuration, observed within the first resonance lines of the alkali-metal atoms. The resonance manifests itself as a narrow feature in the atomic fluorescence or absorption in degenerate conditions, when the magnetic field is varied around the zero value [19].

For alkali-metal atoms contained in uncoated optical cells, the magneto-optical resonance width is limited by the atom transit time through the laser beam. Due to this condition, the linewidth of the resonance is of the order of 10 μT [13]. In case of coated cells, instead, the resonance width is limited by the time $\tau_c = R_c/(2\mathrm{v}_T)$, multiplied by the number N of atomic collisions against the cell wall, without modifications of the atomic internal state. Therefore, the average coherence lifetime is enhanced by a factor N. As a consequence, the spectral width of the Hanle resonances observed in coated cells can be well below 0.1 μT [20]. Indeed, in the case of coated cells, after each collision against the walls the atoms get a Maxwell velocity distribution and, with probability $\varepsilon = 1/N \ll 1$, regain an equilibrium state with random alignment.

1. Cs D_2 line

Simulations are performed in different conditions in order to investigate the Hanle EIT resonance characteristics and their relationship with the antirelaxation coatings and the amount of optical pumping, in the case of Cs D_2 fluorescence (Fig. 2). It is worth recalling here that according to the cesium hyperfine structure, the efficiency of optical pumping is high.

For low-quality antirelaxation coatings, i.e., with $\varepsilon = 0.1$ (Fig. 2, left), the EIT resonance width is still large ($\Delta\nu = 7.2$ μT, with resonance contrast $c = 14.9\%$). An order of magnitude improvement in the quality of the cell coating ($\varepsilon = 0.01$) results in a significant resonance narrowing. For a very good coating ($\varepsilon = 0.001$), the resonance width is reduced to $\Delta\nu = 0.13$ μT.

Unfortunately, due to the efficient optical pumping to the ground-state hyperfine level noninteracting with the laser light, the Cs vapor fluorescence decreases more than 25 times. For an extremely high-quality cell coating ($\varepsilon = 0.00001$, Fig. 2, right), the magneto-optical resonance width is further reduced by an order of magnitude ($\Delta\nu = 0.013$ μT, with resonance contrast $c = 19.8\%$), but at the expense of an additional fluorescence intensity decrease by more than two orders of magnitude with respect to Fig. 2, left.

Generally speaking, the theoretical analysis performed for the D_2 line of Cs shows that the use of an optical cell with

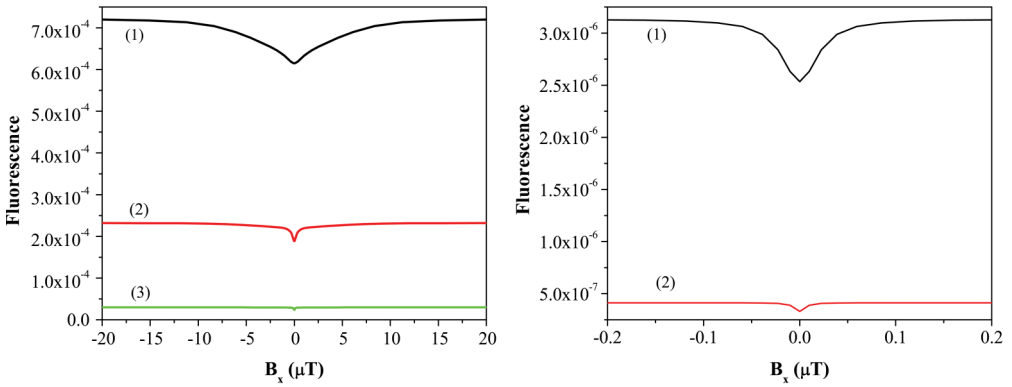

FIG. 2. (Color online) Theoretical Hanle EIT resonance profiles for the Cs $F_g = 4 \rightarrow F_e = 4$ transition for different values ε of the probability of randomization of atomic spin orientation due to atom collision with the cell coated walls. Left: (1) Black trace $\varepsilon = 0.1$, (2) red trace $\varepsilon = 0.01$, (3) green trace $\varepsilon = 0.001$. Right: (1) Black trace $\varepsilon = 0.0001$, (2) red trace $\varepsilon = 0.00001$. Cell radius $R_c = 1.1$ cm, beam radius $R_b = 0.25$ cm, laser power $W = 128$ μW, that is, 652 μW/cm^2.

extremely good coating can provide very narrow magneto-optical resonance. However, due to the strong hyperfine optical pumping, the intensity of the fluorescence dramatically decreases. The high efficiency of the optical pumping in Cs vapor is due to the large frequency difference between the ground-state hyperfine structure levels compared to the Doppler width of the hyperfine optical transitions.

This theoretical result is consistent with numerous experimental evidences and it is supported, in particular, by the observation that the absorption by the Cs atoms in the coated cell is 30 times less than that in the uncoated one under similar experimental conditions [21]. Thus, even if it provides a strong narrowing of the resonance profile, the use of antirelaxation coatings in the case of Cs leads to severe reduction of the resonance amplitude.

2. *K D_1 line*

In the following, results about ^{39}K will be presented. We will refer only to the most abundant isotope 39, and hence the superscript will be omitted. In this case, the situation described in the previous section is different: here, the hyperfine splitting between the two ground levels is $\Delta\nu_{\rm hf} = 462$ MHz, while the Doppler width of the D_1 hyperfine transition is 770 MHz at $T = 300$ K. Under such conditions, the hyperfine optical pumping to the ground-state hyperfine level that is not resonantly excited by the laser light can be much smaller than in the case of Cs. The suppression of optical pumping depends on the amount of velocity-changing collisions (VCCs) of the alkali-metal atoms with the coated cell walls. In fact, even with a narrow-band laser excitation, some repumping to the resonantly excited ground level will take place due to the excitation in the wing of the second hyperfine transition [14].

With an antirelaxation coating, such collisions do not change the atomic spin polarization, but they restore the Maxwell velocity distribution of K atoms in the entire cell volume, thus reducing the optical pumping to the nonresonant level. In other words, thanks to the antirelaxation coating, in K it is possible to take advantage of the VCCs to reduce losses due to optical pumping.

Figure 3 shows the results of the numerical simulations, in the case of the K D_1 line. For a very low quality cell coating (ε=0.1, Fig. 3, left), the fluorescence magneto-optical resonance width is large ($\Delta\nu$=14 μT) and the resonance contrast is 16.2%. Note that for extremely low quality cell

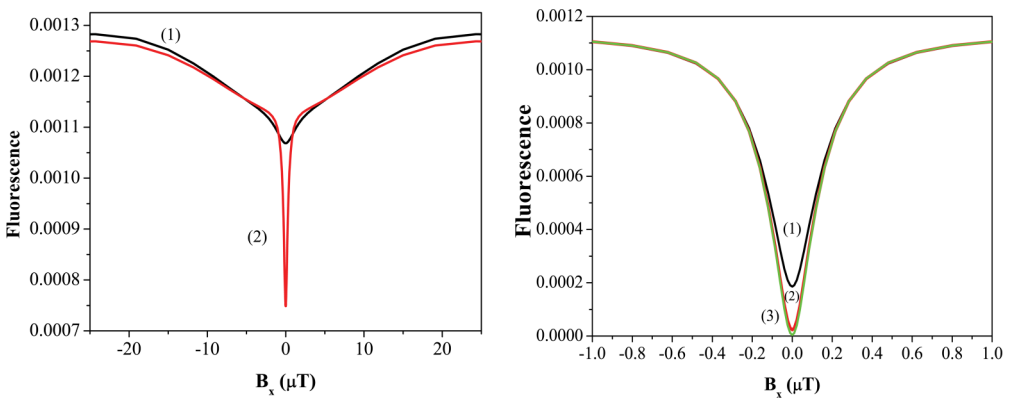

FIG. 3. (Color online) Theoretical Hanle EIT resonance profiles for the K D_1 line for different values ε of the probability of randomization of atomic spin orientation due to atom collision with the cell coated walls. Left: (1) $\varepsilon = 0.1$, (2) $\varepsilon = 0.01$. Right: (1) $\varepsilon = 0.001$, (2) $\varepsilon = 0.0001$, (3) $\varepsilon = 0.00001$. Cell radius $R_c = 1.1$ cm, beam radius $R_b = 0.25$ cm, laser power $W = 128$; μW, that is, 652 μW/cm^2.

TABLE I. Simulation of EIT resonances on the Cs D_2 line and ^{39}K D_1 line: Theoretical EIT contrasts.

ε	Cs D_2 contrast (%)	^{39}K D_1 contrast (%)
0.1	14.9	16.2
0.01	18.0	40.7
0.001	20.0	82.8
0.0001	18.9	97.5
0.00001	19.8	98.6

coating, the magneto-optical resonance contrast is similar for both Cs and K.

An order of magnitude enhancement of the coating quality ($\varepsilon = 0.01$) results instead in the formation of a much narrower Hanle resonance (with $\Delta\nu = 0.6\ \mu$T), superimposed on a broader one (Fig. 3, left). In addition, the contrast of the narrow resonance is 40.7%. It is worth noting that the narrowing of the EIT peak and the enhancement of its contrast are produced by the simultaneous contributions of the antidepolarization coating and VCCs, as observed in Ref. [14]. The composite structure of the resonance is produced by the long-living coherences permitted by the coating. Indeed, a similar behavior has been observed in Rb [15] and in Na with multimode excitation [12], and it was explained with a Ramsey-like induced narrowing produced by multiple interactions of polarized atoms with the resonant laser beam. A further enhancement of coating quality ($\varepsilon = 0.001$) produces a twofold resonance narrowing ($\Delta\nu = 0.3\ \mu$T) and a dramatic increase of the Hanle EIT contrast, up to 82.8%, without a significant reduction of the fluorescence signal. The coating with $\varepsilon = 0.001$ is one of the best that is typically realized in practice. For the smallest value of $\varepsilon = 0.00001$ (Fig. 3, right), the resonance contrast approaches 100% with no significant reduction of the fluorescence signal. The results are summarized in Table I for both Cs and K.

A remarkable result obtained by our model is the reproduction of the different behaviors of Cs and K: indeed, the two alkali-metal species can have completely different behaviors with the enhancement of the quality of the optical cell coating. More specifically, the improvement of the quality of coating in the case of Cs results in a dramatic reduction of resonance signal, while this is the opposite for K. In case the of Cs, see Ref. [21], even with the lower efficiency PDMS coating with respect to the paraffin one, the coherent population trapping resonance amplitude is strongly reduced in the coated cell as compared to the uncoated one. The resonance amplitude reduction is due to the hyperfine optical pumping: atoms excited by the laser light from one ground-state hyperfine level are accumulated to the other ground level, noninteracting with the light. For an uncoated cell, each atomic collision with the cell wall results in spin randomization, while the more efficient the cell coating is, the longer the atom stays at the level noninteracting with the light. As a result of this process, the population of the light-excited level is depleted. From the theoretical analysis, one can conclude that while the Cs D_2 line can provide probably the lowest width of magneto-optical resonance in alkali, K vapor is advantageous due to the large contrast-to-width ratio of magneto-optical resonance and the high absolute value of the resonance amplitude. The slightly broader resonance for K can be attributed to the influence of the repumping process. In fact, the "fresh" K atoms repumped to the ground-state level that is in exact resonance with the light have a lower degree of spin polarization when entering the laser beam. These results are consistent with independent experimental observations [13,14].

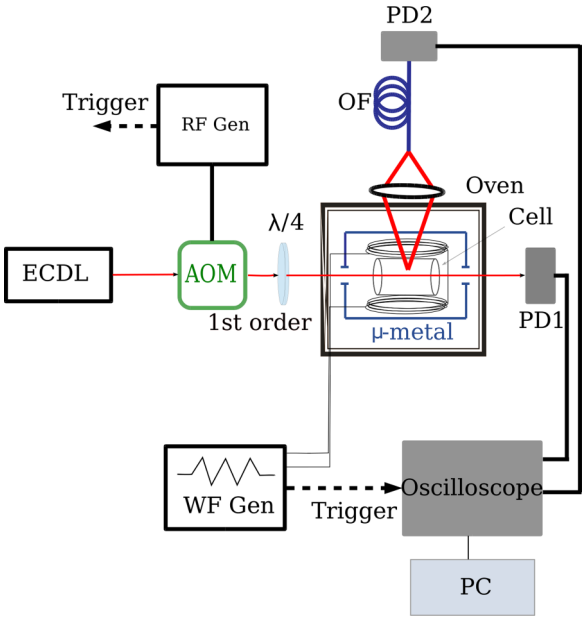

FIG. 4. (Color online) Sketch of the experimental apparatus. WF Gen: Helmholtz coils controls; PD1, PD2: Photodiodes; OF: Optical fiber; AOM: Acousto-optic modulator; RF Gen: AOM driver.

III. EXPERIMENT

Because the influence of optical cell coating to the magneto-optical resonances experimentally measured in Cs has been reported in a previous work [21], here we present in more detail our experimental results related to the case of K atomic vapor. The experimental arrangement is similar to that used in Ref. [14] and is sketched in Fig. 4.

An extended cavity diode laser (ECDL Toptica DL100) is tuned to the D_1 line of K (770 nm). The laser linewidth is of the order of 1 MHz. The maximum output power of the laser is 0.175 mW and the laser beam cross section is 0.02 cm^2. Two types of K cells are used in the experiment: uncoated and coated by a PDMS film. Both (coated and uncoated) cells are of cylindrical shape and have the same dimensions, with side arms containing the alkali-metal reservoir. The reservoir is connected to the cell volume containing only atomic vapor by means of a 1-mm-diameter capillary. The PDMS coating preserves the atomic spin orientation after about 1×10^3 collisions of K atoms with the cell walls. K atoms are irradiated by circularly polarized light tuned to the maximum of the D_1 profile. The optical cell is heated and shielded against stray magnetic fields by inserting it into a μ-metal cylinder. A pair of supplementary Helmholtz coils placed inside the shield produces a magnetic field B orthogonal to the laser beam propagation direction. The current of the coils is swept by means of a tunable power supply driven by a triangular

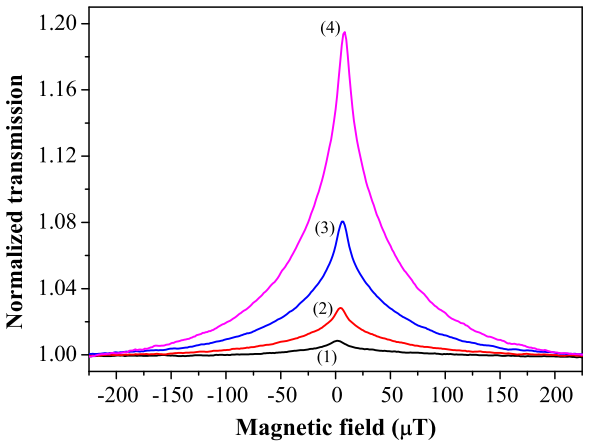

FIG. 5. (Color online) Hanle EIT resonances observed in uncoated cell on the K D_1 line transmission at different temperatures T: (1) =33 °C, (2) =42 °C, (3) =52 °C, (4) =62 °C. Laser power density $I = 8.75\ \mathrm{mW/cm^2}$, with circular polarization.

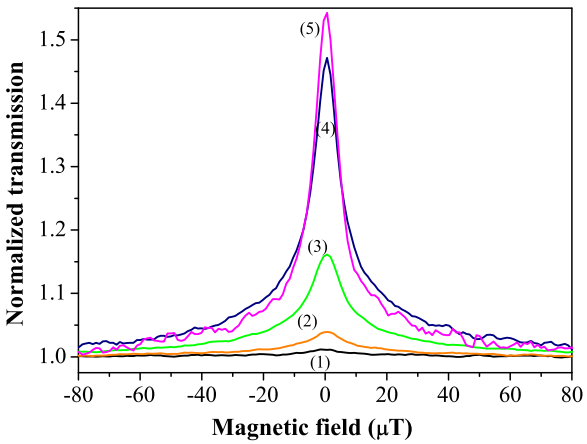

FIG. 6. (Color online) Hanle EIT resonances observed in coated cell on the K D_1 line transmission at different temperatures T: (1) =29 °C; (2) =39 °C; (3) =49 °C; (4) =58 °C; (5) =68 °C. Laser power density $I = 8.75\ \mathrm{mW/cm^2}$, with circular polarization.

waveform. The laser light transmitted through the cell is measured as a function of the magnetic field B, varied around $B = 0$. At the same, time we collect the fluorescence emitted perpendicularly to the laser beam by focusing the light on an optical fiber. In these experimental conditions we observed EIT resonances in the Hanle configuration [14].

In a second experiment, described in Sec. III B, the EIT resonance is produced by amplitude-modulated laser light in nondegenerate conditions, i.e., at nonzero magnetic filed. An acousto-optic modulator is therefore inserted in the apparatus.

A. Hanle EIT in K

Figure 5 presents the magneto-optical resonance profiles observed in uncoated cells, at four temperatures of the atomic source: electromagnetically induced transparency is produced at $B \sim 0$. At each temperature, the laser beam transmission is normalized to its value measured when the magnetic field is detuned well outside of the resonance. With the enhancement of the atomic density, the resonance contrast increases. Typically, the observed width of the resonance is about 40 μT. The shape of the resonance profile is in agreement with the theoretical one, simulated for cells with very low quality of antirelaxation coating (Fig. 3, left: $\varepsilon = 0.1$).

Without changing the experimental conditions, the uncoated cell is replaced by a PDMS-coated one. Both uncoated and coated cells have similar dimensions and geometry. Figure 6 presents the EIT resonance profiles observed in the coated cell transmission for five different atomic source temperatures. The strong narrowing of the Hanle EIT resonance profile in the coated cell is evident. Typically, the width of the resonance is about 1 μT: this means that in the coated cell the resonances are 40 times narrower than in the uncoated one. Note that, in very good agreement with theoretical modeling, together with the resonance narrowing, a strong rising of its contrast takes place (more than twofold).

Together with the absorption signal, we collect also the fluorescence, which, as expected, exhibits a consistent behavior. Indeed, the level of the fluorescence and its spectral profile is proportional to that of the absorbed light. In Fig. 7, the experimental profiles of the EIT resonance obtained at three different temperatures are compared with the theoretical profile. Simulation and experimental data are in qualitative agreement: the simulated resonance exhibits a slightly larger contrast and smaller width than the experimental one. We attribute this effect to the absorption by K atoms, which produces a decrease in the laser intensity along the main axis. In the theoretical modeling, instead, the laser light intensity along the cell was assumed constant.

This is confirmed by the plot presented in Fig. 8: the EIT resonances FWHMs are plotted as a function of the light intensity, in the case of the uncoated cell. Accordingly, the theoretical simulation is performed with $\varepsilon = 1$. The agreement between the data and theory is good; in particular, the behavior with increasing light power is perfectly reproduced.

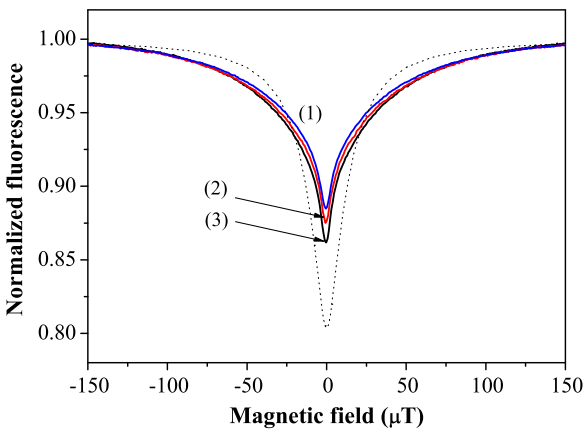

FIG. 7. (Color online) Experimental Hanle EIT resonances in the fluorescence of K atoms in uncoated cell, for different atomic source temperatures T and comparison with the theoretical simulation. (1) blue trace: experimental data $T = 69$ °C; (2) red trace: experimental data $T = 59$ °C; (3) black trace: experimental data $T = 50$ °C. Dotted line: theoretical simulation $T = 60$ °C. Laser power density $I = 4.58\ \mathrm{mW/cm^2}$, for the experiment and theory.

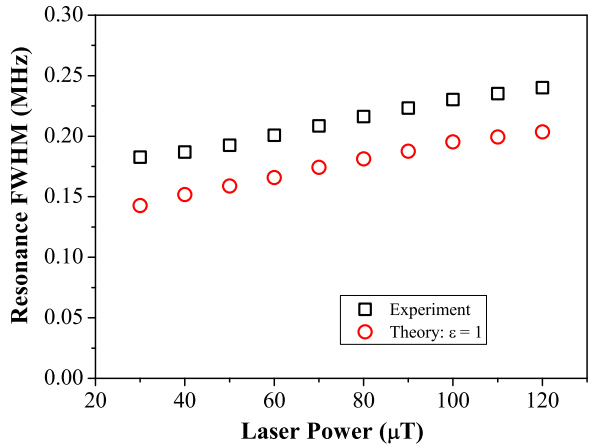

FIG. 8. (Color online) Experimental and theoretical spectral FWHM of the Hanle EIT resonance observed in the fluorescence of K atoms in an uncoated cell, as a function of laser light power, with circular polarization. $T = 75\,^{\circ}\mathrm{C}$. The laser beam area was $s = 0.036\,\mathrm{cm}^2$.

A systematic difference of about $\leqslant 20\%$ in the FWHM is, however, observed, as already anticipated in the case of Fig. 7.

B. EIT on degenerate and nondegenerate levels in K

In this section, we present the results of an experiment in K vapor in which combined EIT resonances are observed in the Hanle configuration and in the classical three-level Λ configuration in nondegenerate conditions, i.e., with a nonzero magnetic field. In the last case, the EIT resonance is prepared by coupling two nondegenerate Zeeman sublevels of a single hyperfine ground level to a common excited level. The two coherent light fields needed for the observation of such a resonance can be produced by laser light modulation either in frequency [22] or in amplitude [14] in the kHz or MHz bands.

In our case, the amplitude modulation was chosen as more practical for potassium and with less stringent requirements for the control electronics. The resonant laser light was therefore modulated by an acousto-optical modulator (AOM) at a constant frequency f of the order of hundreds of kHZ to MHz. After the AOM, the first-order beam was circularly polarized and directed to the atomic sample under investigation, as in the experiment described in the previous section. While the frequency f was kept constant, the magnetic field was varied in a suitable interval around $B = 0$ by a triangular waveform. In this way, the three-peak structures shown in Figs. 9 were obtained: whenever the magnetic field value reaches the resonant condition $B = \pm f_{\mathrm{Larmor}}/k$, where $k = 7\,\mathrm{kHz}/\mu\mathrm{T}$ and f_{Larmor} is the Larmor frequency of the atomic precession in the external magnetic field, the coherent coupling between the nondegenerate Zeeman sublevels produces the two lateral peaks. In addition, a central resonance corresponding to the EIT resonance based on degenerate Zeeman sublevels is observed at $B = 0$. For more details of the experimental arrangement, see [14].

Figure 9 (left) presents the experimental results obtained for the uncoated optical cell containing K vapor, at four different temperatures. As well as the nonmodulated light case and in agreement with theoretical profile, the width of the EIT resonance on degenerate Zeeman sublevels is several hundred kHz. The two EITs on nondegenerate sublevel resonances, centered at ± 3.93 MHz, corresponding to $B = \pm 560\ \mu$T, are two times broader and their contrast is about seven times less than that of the central resonance. In Figure 9 (right), the case of the coated cell is shown. The contrast predicted by the theory is five times larger ifor the coated cell than for the uncoated one, for the EIT on degenerate sublevels. Accordingly, in the experiment we observe in the coated cell a 4 times greater contrast than in the uncoated one. In addition, our model predicts a reduction of the width of the degenerate EIT resonance in coated cells by a factor of 47 compared to the ones in uncoated cells. Indeed, consistently with the predictions and the general mechanisms highlighted by the theoretical model, the experimental data exhibit a 45 times reduction of EIT resonance width using the coated cell. Similar narrowing of the EIT resonances based on nondegenerate levels is also observed. Moreover, in the coated cell, both types of resonance have similar spectral widths. It is worth noting that deviations between the simulations and the experimental results similar to the ones described in Figs. 7 and 8 were observed also

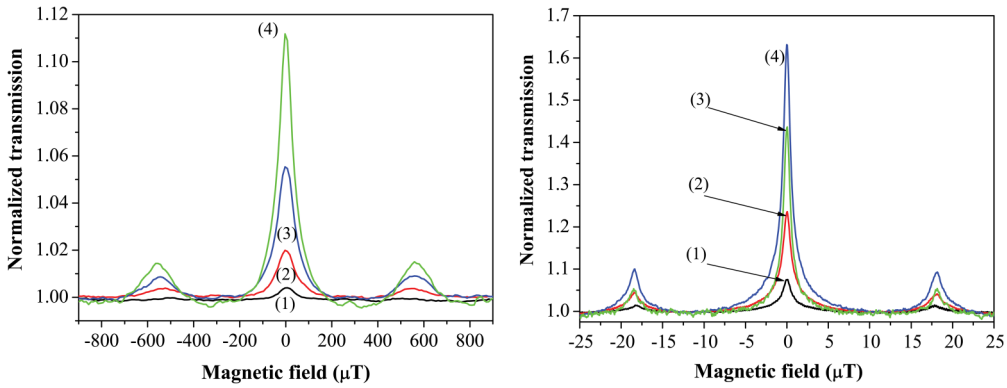

FIG. 9. (Color online) Left: K EIT resonances on degenerate and nondegenerate levels observed in uncoated cell with amplitude modulated laser light ($f = 3.93\,\mathrm{MHz}$), for different atomic source temperatures T: (1) $=47\,^{\circ}\mathrm{C}$, (2) $=58\,^{\circ}\mathrm{C}$, (3) $=68\,^{\circ}\mathrm{C}$, (4) $=77\,^{\circ}\mathrm{C}$. Laser power density $I = 8.75\,\mathrm{mW}/\mathrm{cm}^2$, with circular polarization. Right: K EIT resonances on degenerate and nondegenerate levels observed in PDMS coated cell with amplitude modulated laser light ($f = 128\,\mathrm{kHz}$), for different atomic source temperatures T: (1) $=43\,^{\circ}\mathrm{C}$, (2) $=52\,^{\circ}\mathrm{C}$, (3) $=63\,^{\circ}\mathrm{C}$, (4) $=70\,^{\circ}\mathrm{C}$. Laser power density $I = 8.75\,\mathrm{mW}/\mathrm{cm}^2$, with circular polarization.

in this case. The theoretical model correctly reproduces the observations, with the exception of a systematic difference in the calculated widths, which is independent of the mechanisms for the realization of the EIT resonances. This further supports the hypothesis that the discrepancy is caused by the decrease of the laser intensity during propagation in the atomic vapor. In summary, the use of a coated cell filled with K vapor is also advantageous for EIT resonance preparation by modulated light, in terms of contrast and width.

Concerning the practical applications of antirelaxation coatings, our previous study [14] has shown that for EIT observation in coated cells, the optimal atomic source temperature is around $T = 50\,^{\circ}\mathrm{C}$. Under such conditions, the resonance contrast is $C = 50\%$, with a very good signal-to-noise ratio. Further increasing of K density and, therefore, of the operational temperature results in its reduction.

In the case of K, paraffin is not suitable because of its low working temperature ($T < 40\,^{\circ}\mathrm{C}$). However, PDMS was proven to operate very well up to $T = 80\,^{\circ}\mathrm{C}$. Moreover, the use of light-induced atomic desorption (LIAD) with visible light provides a nonthermal technique to increase and stabilize the vapor density in the presence of antirelaxation coatings. In this way, the cell temperature can be decreased well below $T = 50\,^{\circ}\mathrm{C}$ for EIT experiments [23].

Cs vapor in buffered cells was successfully used for development of an optical magnetometer based on nonlinear magneto-optical rotation in a two-channel configuration [24]. A pump-probe approach by two lasers has been proposed with wide frequency modulation of the pump laser, with the purpose of producing both synchronous Zeeman optical pumping and hyperfine repumping to the working hyperfine level. In addition, Cs cells are kept at around $T = 30\,^{\circ}\mathrm{C}$ (using circulating hot water), in order to increase the signal/noise ratio.

Finally, in Ref. [25], it has been demonstrated that octadecyltrichlorosilane (OTS) allows potassium or rubidium atoms to experience hundreds of collisions with the cell walls before depolarization, and that an OTS coating remains effective up to about $T = 170\,^{\circ}\mathrm{C}$ for both potassium and rubidium. The practical use of the OTS coated cells has been demonstrated in high-density alkali-metal magnetometry, showing that such cells permit narrow magnetic resonance linewidths and larger optical rotation signals than buffer-gas-filled cells under similar operating conditions.

IV. CONCLUSIONS

A new theoretical model is presented for the analysis of magneto-optical resonances in alkali-metal atoms in the presence of antirelaxation coatings with different efficiencies and, therefore, different impacts of hyperfine optical pumping. In particular, the formation of EIT resonances is studied on the D lines of Cs and K by varying a suitable parameter describing the coating efficiency. The approach described here allows one to extend the investigation to highly efficient coatings, which was impossible in previous investigations, such as in Ref. [12].

In the case of Cs, the hyperfine splitting of the ground level is much larger than the Doppler widths of the corresponding optical transitions. Consequently, as demonstrated by the agreement of our simulation with previous experimental results [21], a highly efficient antirelaxation coating used for narrowing the EIT resonance leads to a complete depletion of the ground level excited by the monomode laser light, as a consequence of hyperfine optical pumping. Indeed, the EIT resonance amplitude decreases by three orders of magnitude, even if the resonance width decreases below 0.1 μT.

For K, the behavior is opposite, as shown by the experimental results in the Hanle and in the nondegenerate configuration with amplitude modulated light. Here, in fact, as observed also in previous works [14], the EIT resonance is enhanced in the presence of efficient coatings. Indeed, the K D_1 line hyperfine ground-state splitting is smaller than the Doppler broadening of the corresponding optical transitions. Therefore, a partial compensation of hyperfine optical pumping naturally occurs. This phenomenon, as our model demonstrates, becomes relevant in coated cells, as the result of numerous atom-wall collisions without atomic spin randomization. The "repumping" effect is further enhanced by the Maxwellization of the atomic velocity distribution provided by velocity-changing collisions of atoms with the coated cell walls. As the model confirms, this process leads to an increase of the EIT resonance amplitude with an efficient coating, even if it produces broadening of the resonance, as a consequence of the nonpolarized atoms in the hyperfine ground level noninteracting with the light.

In the experiment with K, the temperature range here investigated corresponds to atomic densities between $\sim 5 \times 10^9$ and $\sim 8 \times 10^{10}$ cm^{-3}. In the case of Cs, instead, the same temperature range corresponds to an almost two order of magnitude higher vapor density. Hence, in experiments based on linear absorption, at low temperature, it is advantageous to use Cs vapor: given the low light intensity required for linear atom-laser interaction, the hyperfine optical pumping has a small impact.

In the case of nonlinear optical processes and, in particular, of coherent resonances whose qualities are measured by the ratio of the contrast over their widths, the narrowing of the resonance requires the use of optical cells with a buffer gas or an antirelaxation coating. However, as this causes a dramatic reduction of the resonance amplitude due to the efficient hyperfine optical pumping, the use of K vapor is advantageous in those experiments.

ACKNOWLEDGMENTS

This work was partially supported by the Bilateral Cooperation Agreement between the Italian National Council of Research (CNR) and the Bulgarian Academy of Sciences (BAS), Common projects 2013-2015 and Marie Curie International Research Staff Exchange Scheme Fellowship within the 7th European Community Framework Programme: "Coherent optics sensors for medical applications-COSMA" (Grant Agreement No. PIRSES-GA-2012-295264). L.M. was supported by an UCL Quantum Science and Technology Institute (UCLQ) Fellowship.

APPENDIX: LIGHT-ATOM INTERACTION MODEL

In this Appendix, our method of numerical solution of equations related to resonant interaction of polarized radiation with alkali-metal atoms is briefly described. The dynamics of alkali-metal atoms in external magnetic and the electric field

of a laser beam is described by the density matrix equation ρ:

$$i\hbar\left(\frac{\partial}{\partial t}+\mathbf{v}\frac{\partial}{\partial \mathbf{r}}+\hat{\Gamma}\right)=[H_0,\rho]+[V_B+V,\rho]. \tag{A1}$$

Here, $\mathbf{r}$ and $\mathbf{v}$ are position and velocity of an atom, $\hat{\Gamma}$ is the atomic relaxation operator, comprising the spontaneous decay of excited states. H_0 is the free-atom Hamiltonian, $V_B=\mu g\mathbf{F}\cdot\mathbf{B}$ is the interaction potential of an atom with the magnetic field $\mathbf{B}$, where $\mathbf{F}$ is the atomic angular momentum, g is the Landé factor, and μ the Bohr magneton. The interaction of the atom with the electrical field of the laser light $\mathbf{E}$ is considered in the dipole approximation $V=-\mathbf{d}\cdot\mathbf{E}$, where $\mathbf{d}$ is the atomic dipole moment. The light induces optical transitions between ground-state levels $g=|F_g,M_g\rangle$ and excited-state levels $e=|F_e,M_e\rangle$, where M is the total angular momentum projection on the quantization axis.

The electric field of the laser light is described in the following form:

$$\mathbf{E}=\mathbf{E}_0e^{-i\omega t+i\mathbf{k}\cdot\mathbf{r}}+\text{c.c.}, \tag{A2}$$

where $\mathbf{E}_0$ is the polarization vector of the light. We take into consideration an atom with a set of excited states $\{|e\rangle=|F_e,M_e\rangle\}$ with energies $\{E_e\}$ and with a set of ground-state levels $\{|g\rangle=|F_g,M_g\rangle\}$ with energies $\{E_g\}$. For instance, four excited and two ground levels participate in transitions of the D_2 line of alkali-metal atoms in the hyperfine interaction approximation. Equation (A1) retains only the resonant terms of interaction with radiation (rotating-wave approximation).

The matrix element of the electric dipole interaction thus can be written as

$$V_{eg}=-\sum_{\sigma}(-1)^{\sigma}\langle e|d_{-\sigma}|g\rangle E_{\sigma},\quad V_{ge}=V_{eg}^{*}, \tag{A3}$$

where d_σ and E_σ are the circular components of the vectors of the dipole moment and the electric field of the wave ($\sigma=-1,0,+1$). The explicit form of the matrix element of the dipole moment thus is

$$\begin{aligned}\langle F_e,M_e|d_\sigma|F_g,M_g\rangle &= d(-1)^{F_e-M_e+J_e+I+F_g+1}\\ &\times\sqrt{(2F_e+1)(2F_g+1)}\begin{Bmatrix}J_e & F_e & I\\ F_g & J_g & 1\end{Bmatrix}\\ &\times\begin{pmatrix}F_e & 1 & F_g\\ -M_e & \sigma & M_g\end{pmatrix}.\end{aligned} \tag{A4}$$

Here, d is the reduced matrix element of the dipole moment of the optical transition $J_g\to J_e$, where $J_{e,g}$ are the total electron moment of excited and ground states, respectively, and I is the nuclear moment. {} indicate the $3J$ symbols and () are the Clebsch-Gordan coefficients.

The matrix element of the potential in the presence of interaction with the magnetic field has the form, if $F_g=F_e=F$,

$$\begin{aligned}V_B(FM_1|FM_2) &= \sum_{\sigma}\mu_{e,g}B_\sigma(-1)^{F+M_2-2M_1+1}\sqrt{\frac{2F+1}{(F+1)F}}\\ &\times\frac{I(I+1)-J_{e,g}(J_{e,g}+1)-F(F+1)}{2}\\ &\times\begin{pmatrix}F & 1 & F\\ -M_1 & \sigma & M_2\end{pmatrix}.\end{aligned} \tag{A5}$$

In turn, $\mu_{e,g}$ is calculated via the electron Landé factor as

$$\mu_{e,g}=\mu\left(1+\frac{J_{e,g}(J_{e,g}+1)-L_{e,g}(L_{e,g}+1)+S(S+1)}{2J_{e,g}(J_{e,g}+1)}\right). \tag{A6}$$

It is worth recalling here that for the D_2 line, $J_e=3/2$; while for the D_1, $J_e=1/2$. The ground state has an angular momentum $J_g=1/2$. $L_e=1$ and $L_g=0$ are the electron orbital angular momenta for the excited and ground states respectively. μ is the Bohr magneton. In this way, the potential of interaction with the magnetic field has only diagonal (in terms of the energy states) nonzero matrix elements.

Finally, we compute the relaxation operator for the case of purely spontaneous decay. For the excited states, we obtain

$$(\hat{\Gamma}\rho)(F_e,M_e|F_e',M_e')=\gamma\rho(F_e,M_e|F_e',M_e'), \tag{A7}$$

where γ is the spontaneous decay rate, as experimentally determined. In the case of the nondiagonal elements of the matrix, instead, we have

$$(\hat{\Gamma}\rho)(F_e,M_e|F_g,M_g)=\frac{\gamma}{2}\rho(F_e,M_e|F_g,M_g). \tag{A8}$$

For the ground state, the term has a more complicated form:

$$\begin{aligned}&(\hat{\Gamma}\rho)(F_g,M_g|F_g',M_g')\\ &=\delta_{F_g,F_g'}\frac{\gamma}{d^2}\sum_{\sigma,F_e,M_e,M_e'}\langle F_g,M_g|d_\sigma|F_e,M_e\rangle\\ &\times\langle F_e,M_e'|d_{-\sigma}|F_g,M_g'\rangle\rho(F_e,M_e|F_e,M_e').\end{aligned} \tag{A9}$$

In this way, all the operators involved in Eq. (A1) are determined. Then, Eq. (A1) has to be solved along straight lines crossing the laser beam, which has a Gaussian profile with beam radius r_b:

$$I(r)=I_0e^{-r^2/r_b^2}. \tag{A10}$$

The value of I_0 is assumed constant along the longitudinal dimension of the optical cell containing the alkali-metal vapor.

To solve the problem numerically, it is customary to transform Eq. (A1) in a system of linear equations of the form

$$\frac{d}{dt}\rho+U\rho=0, \tag{A11}$$

where ρ is no longer a matrix, but a vector instead. U is a matrix matching the size of the vector. For more details, see Ref. [17].

Experiments aimed to investigate the interaction of polarized radiation with alkali-metal vapors usually involve the measurement of the intensity of the resonant laser beam after the optical cell, or the intensity of fluorescence emitted in a direction orthogonal to the laser beam. From the point of view of the present treatment, both these methods are almost equivalent, with the only difference that the peak in fluorescence corresponds to the dip in the power of transmitted radiation and vice versa.

In this paper, we calculate the fluorescence intensity by the formula

$$I_{fl}(\mathbf{n})=A\langle[\mathbf{n}\times\mathbf{d}]^2\rho\rangle_{e,r_p,\mathbf{v}}, \tag{A12}$$

where **n** is the versor indicating the direction of observation of the fluorescence, and A is an empirical factor taking into account the spontaneous decay rate, the geometry of the experimental setup, and so on. In this equation, averaging over all the atomic excited states, velocities, and impact parameters r_p is performed. It is worth noting that, in this case, the fluorescence intensity depends on the angle between the observation direction and the laser beam propagation direction.

In evacuated cells, both coated and uncoated, we neglect the velocity-changing collisions either inside or outside the laser beam; the only velocity-changing collisions taken into account are the ones against the coated walls of the glass cell. We assume, in fact, that after numerous collisions with the walls, atoms gain a Maxwellian velocity distribution.

It is worth recalling that, nevertheless, in the case of very good coatings, the inner states of the atom remain unaffected with high probability. On the contrary, in the case of background or buffer gas inside the cell, the velocity-changing collisions between the alkali-metal atoms and the buffer gas are not necessarily negligible and should thus be taken into account, as reported in Ref. [26], where only collisions in the volume not occupied by the laser beam are considered.

[1] F. Kh. Gel'mukhanov and A. M. Shalagin, Pis'ma Zh. Eksp. Teor. Fiz. **29**, 773 (1979) [JETP Lett. **29**, 711 (1979)].

[2] E. B. Alexandrov, M. V. Balabas, D. Budker, D. English, D. F. Kimball, C.-H. Li, and V. V. Yashchuk, Phys. Rev. A **66**, 042903 (2002).

[3] S. Gozzini and A. Lucchesini, Eur. Phys. J. D **28**, 157 (2004).

[4] E. Breschi, G. Kazakov, C. Schori, G. Di Domenico, G. Mileti, A. Litvinov, and B. Matisov, Phys. Rev. A **82**, 063810 (2010).

[5] W. Hansel, P. Hommelhoff, T. W. Hansch, and J. Reichel, Nature **413**, 498 (2001).

[6] S. Du, M. B. Squires, Y. Imai, L. Czaia, R. A. Saravanan, V. Bright, J. Reichel, T. W. Hänsch, and D. Z. Anderson, Phys. Rev. A **70**, 053606 (2004).

[7] C. Klempt, T. van Zoest, T. Henninger, O. Topic, E. Rasel, W. Ertmer, and J. Arlt, Phys. Rev. A **73**, 013410 (2006).

[8] D. Budker and M. Romalis, Nat. Phys. **3**, 227 (2007).

[9] M. Auzinsh, D. Budker, and S. Rochester, *Optically Polarized Atoms* (Oxford University Press, Oxford, 2010).

[10] T. Bandi, C. Affolderbach, and G. Mileti, J. Appl. Phys. **111**, 124906 (2012).

[11] M. V. Balabas, T. Karaulanov, M. P. Ledbetter, and D. Budker, Phys. Rev. Lett. **105**, 070801 (2010).

[12] S. Gozzini, L. Marmugi, A. Lucchesini, S. Gateva, S. Cartaleva, and K. Nasyrov, Phys. Rev. A **84**, 013812 (2011).

[13] C. Andreeva, S. Cartaleva, Y. Dancheva, V. Biancalana, A. Burchianti, C. Marinelli, E. Mariotti, L. Moi, and K. Nasyrov, Phys. Rev. A **66**, 012502 (2002).

[14] S. Gozzini, S. Cartaleva, A. Lucchesini, C. Marinelli, L. Marmugi, D. Slavov, and T. Karaulanov, Eur. Phys. J. D **53**, 153 (2009).

[15] S. Gateva, L. Gurdev, E. Alipieva, E. Taskova, and G. Todorov, J. Phys. B **44**, 035401 (2011).

[16] K. Nasyrov, Optoelectron. Instrum. Data Process. **49**, 87 (2013).

[17] K. Nasyrov, Optoelectron. Instrum. Data Process. **46**, 248 (2010).

[18] K. Nasyrov, S. Cartaleva, N. Petrov, V. Biancalana, Y. Dancheva, E. Mariotti, and L. Moi, Phys. Rev. A **74**, 013811 (2006).

[19] F. Renzoni, W. Maichen, L. Windholz, and E. Arimondo, Phys. Rev. A **55**, 3710 (1997).

[20] N. Castagna, G. Bison, G. Di Domenico, A. Hofer, P. Knowles, C. Macchione, H. Saudan, and A. Weis, Appl. Phys. B **96**, 763 (2009).

[21] G. Bevilacqua, V. Biancalana, E. Breschi, Y. Dancheva, C. Marinelli, E. Mariotti, L. Moi, C. Andreeva, T. Karaulanov, and S. Cartaleva, Proc. SPIE **5830**, 150 (2005).

[22] C. Andreeva, G. Bevilacqua, V. Biancalana, S. Cartaleva, Y. Dancheva, T. Karaulanov, C. Marinelli, E. Mariotti, and L. Moi, Appl. Phys. B **76**, 667 (2003).

[23] L. Marmugi, S. Gozzini, A. Lucchesini, A. Bogi, A. Burchianti, and C. Marinelli, J. Opt. Soc. Am. B **29**, 2729 (2012).

[24] J. Belfi, G. Bevilacqua, V. Biancalana, S. Cartaleva, Y. Dancheva, K. Khanbekyan, and L. Moi, J. Opt. Soc. Am. B **26**, 910 (2009).

[25] S. J. Seltzer and M. V. Romalis, J. Appl. Phys. **106**, 114905 (2009).

[26] K. Nasyrov and S. Cartaleva, Optoelectron. Instrum. Data Process. **48**, 389 (2012).